Experimental Study of a Normal Shock/Homogeneous Turbulence Interaction

Bruno Auvity, Stéphane Barre, Jean-Paul Bonnet

Proceedings of ASME FEDSM'02
ASME 2002 Fluids Engineering Division Summer Meeting
Montreal, Quebec, Canada, July 14-18, 2002

FEDSM2002-31090

EXPERIMENTAL STUDY OF A NORMAL SHOCK / HOMOGENEOUS TURBULENCE INTERACTION

Bruno AUVITY
LEA/CEAT
43, rue de l'aérodrome
86 036 POITIERS Cedex - FRANCE

Stéphane BARRE
LEGI
1025, rue de la piscine, B.P. 53
38 041 GRENOBLE Cedex 9 - FRANCE

Jean-Paul BONNET
LEA/CEAT
43, rue de l'aérodrome
86 036 POITIERS Cedex - FRANCE

ABSTRACT

The problem of shock wave – turbulence interaction is addressed experimentally in a simplified flow configuration: the shock is normal to the flow direction and the incoming turbulence is homogeneous and quasi-isotropic. This paper mainly deals with the problem of the experimental realization of such an interaction in a supersonic wind tunnel. On the basis of an experimental set-up that showed great aptitude in creating a shock-turbulence interaction pure from major parasitic effects, see Barre et al. (1996), a new turbulence generator and a new shock generator were designed and built. It was found that the new turbulence generator creates a homogenous and quasi-isotropic turbulent supersonic flow at a distance of about 25 mesh sizes. The benefit of this new system was to increase the turbulence level before the interaction with the shock from 0.3 % to 1.7%. The new shock generator system permitted to stabilize a normal shock of larger size compared to the previous configuration, at a distance of 32 mesh sizes. Initial conditions at the shock position were determined with details: important turbulent quantities of the supersonic flow before the interaction, such as turbulent kinetic energy, dissipation rate, Taylor micro-scale and integral length scale, were estimated. With this new experimental set-up, detailed turbulence measurements before and after the shock using fluctuations diagram techniques will be performed.

INTRODUCTION

The study of the basic case of shock interactions with homogeneous and isotropic turbulence can give significant insights into the ubiquitous problem of shock-wave/boundary layer interaction. The experimental realization of such an interaction in a laboratory is a very delicate task. There are actually two problems: the first one is to generate a homogeneous and isotropic flow and the second, to generate an interacting normal shock. There are two classical ways to achieve this goal, either in shock tubes or in supersonic wind tunnel, see Andreopoulos et al. (2000) for a review. When attempts have been made to realize such an interaction in wind tunnel, Jacquin et al. (1991), Debiève and Lacharme (1986), Barre et al. (1996), one common limiting feature of these experimental realizations was the very low level of turbulence. Induced experimental difficulties leaded to difficulties in interpreting the results.

However, results obtained in Barre et al. (1996) were very promising because they showed an amplification of the longitudinal velocity fluctuations across the interaction in agreement with the Linearized Interaction Analysis of Ribner (1954), see figure 1. As it is hard to find a consensus of the experimental results, this experimental configuration has been judged relatively pure in terms of boundary conditions.

Figure 2 shows a sketch of the experimental set-up. The supersonic turbulent field was obtained by placing a multi-nozzle in the wind tunnel. The multi-nozzle is made of 625 (25 x 25) small Mach 3 individual axisymmetric nozzles. The exit section of each nozzle is a 6 x 6 mm^2 square that gives an equivalent mesh size, m, of 6 mm. The multi-nozzle creates a kind of grid turbulence. The shock generator was made of two wedges creating a Mach effect. The two important limitations of this experimental set-up were a too low turbulence level in the homogeneous part of the supersonic flow upstream of the shock, typically 0.3 %, and a normal shock too small in the y direction to be qualified as "infinite", 15 mm to be compared

with a turbulent integral length scale of about 3 mm and the mesh size of 6 mm.

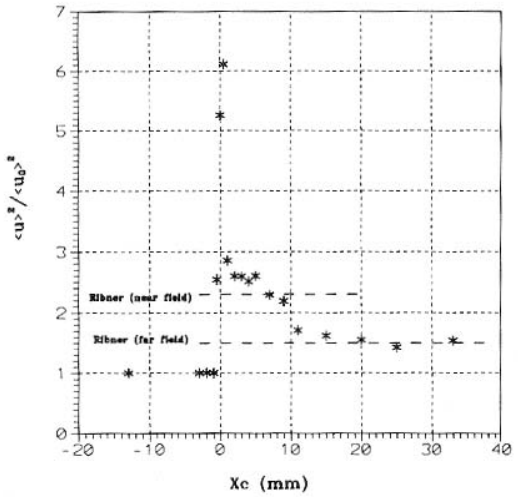

Figure 1: Amplification of the longitudinal velocity fluctuations across the interaction from Barre et al. (1996)

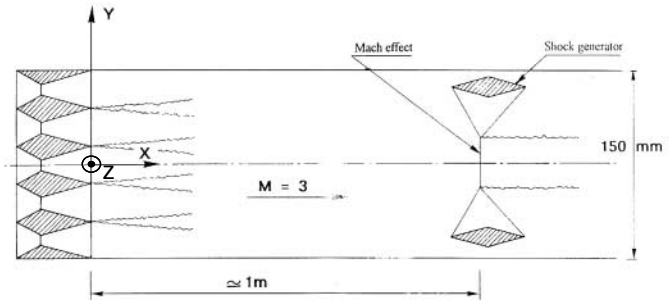

Figure 2: sketch of the previous experimental setup adapted from Barre et al. (1996).

The motivation of the present work was then to improve the flow quality before its interaction with the normal shock (especially increase the fluctuations field) and to generate a larger normal shock compared to local turbulent scales. Additional objective was to decrease the acceleration in the downstream region of the normal shock via an optimum design of the shock generator.

NOMENCLATURE

e: CTA voltage output.
h: inner channel height = 5 mm
l: multi-channel length = 10 x h = 50 mm.
m: mesh size = 6 mm
M: Mach number.
$\frac{1}{2}\cdot q^2$: turbulent kinetic energy
u: longitudinal velocity (X axis)
v: lateral velocity (Y axis)
w: lateral velocity (Z axis)
x: streamwise position
y: spanwise position
z: vertical position
ε: dissipation rate
η: Kolmogorov length-scale
λ: Taylor micro-scale

I. EXPERIMENTAL FACILITY AND APPARATUS

A. Wind tunnel

Experiments were conducted in a square section (150 x 150 mm^2), supersonic wind tunnel driven by a hypersonic ejector (M = 6). The stagnation temperature was stabilized to 270 K and the stagnation pressure was 0.9 x 10^5 Pa. As we will see later, with the introduction of the new turbulence generator, the Mach number in the test section was about 2.1. The resulting unit Reynolds number was about 5.3 x 10^6 m^{-1}.

B. Turbulence generator system

One of the main task was to design a new "turbulence generator" system that could create a supersonic turbulent flow with significant and easily measurable velocity fluctuations. With the multi-nozzle system, turbulence in the downstream supersonic flow was created by the confluence of wakes created by adjacent supersonic divergent nozzles. However, as nozzles were shorts and lips were very thins, wakes were not very marked (the defect velocity on each wake axis was not low enough). Therefore regions of limited shear were generated. The idea here was to enhance the presence of the wakes. We then introduced a plate downstream each lip and we designed what we called a multi-channel system. A square (5 x 5 mm^2) channel followed every divergent supersonic nozzle. As the multi-nozzle, the multi-channel was constituted of 625 channels.

Three important considerations were taken into account for the design of the multi-channel:

- Channel inlet had to be designed to avoid the generation of strong shock waves that could prevent the establishment of supersonic flow in the channel flow.
- In order to allow the development of significant supersonic boundary layers, the multi-channel had to be long enough. On the other hand, a long channel would create a large loss in stagnation pressure and even make the flow subsonic.
- The square divergent nozzle had to be designed to prevent the formation of separated flow that create important Mach waves in the downstream supersonic flow.

Figure 3 presents a sketch of a constitutive element of the assembled "multi-nozzle + multi-channel" system. The channel inlet has a 7° inclination. The total channel length was 10 x h. The divergent nozzle had an angle of 7°. At a distance 2 x h from the channel inlet section, the average Mach number in the square section was estimated to be about 2.5. A In the channel,

the main stream alternately passes through a complex pattern of expansion and shock waves interacting with the boundary layer, so that the Mach number decreased along the channel.

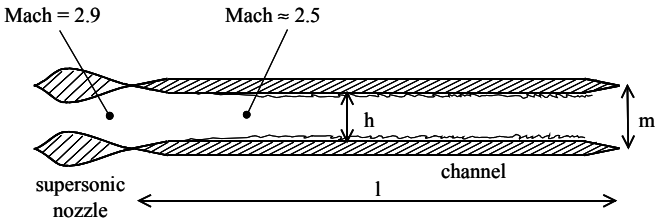

Figure 3: Sketch of an element of the ensemble "multi-nozzle + multi-channel"

C. Hot wire anemometer

Turbulence measurements presented in the paper were performed using constant temperature anemometry. The anemometer was a DANTEC 55 M10 equipped with a standard bridge. The probes were DANTEC 55P11 model with a reduced gap of about 0.7 – 0.8 mm between the prongs and a 2.5 μm platinium-plated tungsten wire. Wires were slightly slacked to avoid parasitic strain gauge effects. The aspect ratio was about 300. Typical bandwidths were greater than 200 kHz.

CTA were operated with high overheat ratio, typically 0.8, because in this condition, CTA was mainly sensitive to mass flux fluctuations. Velocity fluctuations variance was deduced from mass-flux fluctuations variance using the strong Reynolds analogy, Smits and Dussauge (1989). As the Reynolds number did not vary too much in the flow under study (which was mainly composed of far wakes), the resulting uncertainty on longitudinal velocity fluctuations could be estimated to be no more than 10%.

II. QUALIFICATION OF THE SUPERSONIC MEAN FIELD

The introduction of the multi-channel required a new qualification of the downstream supersonic field. Mean quantities (as total pressure, static pressure) were measured using Pitot tube and static pressure probe. Mach waves were visualized using Schlieren device.

Schlieren pictures presented figure 4 revealed the presence of Mach waves emitted from the lips of the multi-channel that are damped with the distance to the multi-channel. The angle between the Mach waves and the horizontal line was about ± 28°, which corresponded to a Mach number of 2.10. This value is significantly smaller than the Mach number of the supersonic flow downstream of the multi-nozzle alone, i.e. 2.85. An important loss of total pressure occurred in the multi-channel. The total pressure in the test section was about 4 x 10^5 Pa with the introduction of the multi-channel whereas it was about 8x 10^5 Pa with the multi-nozzle alone.

A particular feature could be distinguished in the Mach waves pattern. Two dashed white lines that mark the two Mach waves issued from the top and bottom of the multi-channel are reported figure 4(a). These two lines delimits two different region noted 1 and 2. Mach waves included in cone 1 were directly issued from the lips of the multi-channel. Mach waves in cone 2 appeared less intense because they were all reflected once on the test section walls. Their intensities were damped and they changed in nature. As far as the future location of the Mach effect creating the normal shock, the region downstream of the cone 1 had to be considered.

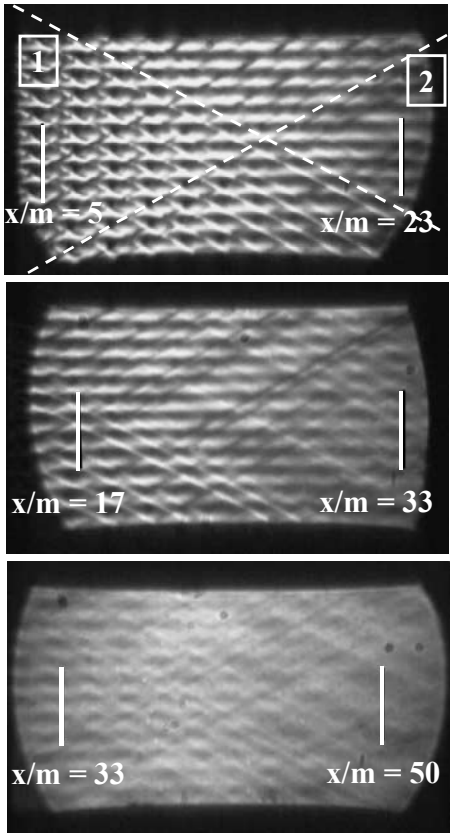

4(a)

4(b)

4(c)

Figure 4: Schlieren pictures (1 ms exposure time) of the supersonic flow downstream of the ensemble "multi-nozzle + multi-channel". (the flow is from left to right)

Spanwise and streamwise repartitions of Mach number in the test section were determined. For each considered streamwise position, pressure probes traversed on at least two mesh sizes to estimate inhomogeneity. Results are shown in figure 5. Square dots correspond to average Mach number for each traverse.

At x/m = 11, measured Mach number was 2.12. This value is in agreement with the estimated value from Mach waves angle figure 4. A slight streamwise evolution of the Mach number could be observed. Mach number decreased from the multi-channel to a streamwise position of about 20 mesh sizes. This deceleration region corresponded to cone 1 shown figure 4(a) where Mach waves were the more intense. They

contributed to a compression of the flow. Downstream of cone 1 (in cone 2), a weak acceleration of the flow was measured. This was because nature of Mach waves changed. They then provoked a weak expansion. The acceleration in cone 2 was observed to be weaker than the deceleration in cone 1. We considered that the flow reached a quasi-equilibrium state as far as pressure was concerned in portion of the flow downstream cone 1.

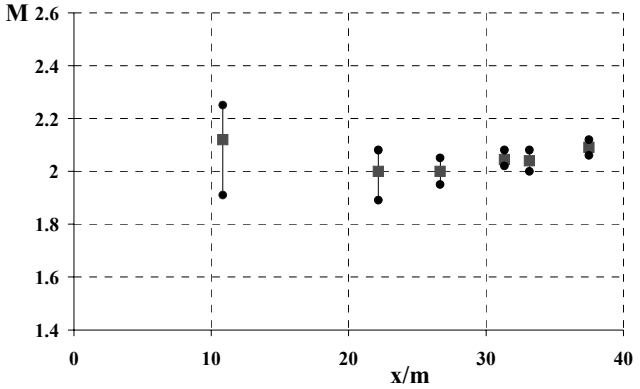

Figure 5: Streamwise evolution of average Mach number (square dots) and lateral dispersion of Mach number (circle dots) in the test section.

The spanwise dispersion of Mach number is shown figure 5. Mach number minima were obtained along the wake lines downstream of the multi-channel lips and the maxima along the channel centerlines of the multi-channel. Up to x/m of about 30, Mach number root-mean square value decreased to less than 1%. Therefore, from x/m of about 30, the supersonic flow was considered to be homogeneous. This value was close to the one observed in grid turbulent subsonic flow, x/m of about 25, see Comte-Bellot and Corssin (1966).

III. QUALIFICATION OF THE SUPERSONIC TURBULENT FIELD

Turbulent field was investigated in several streamwise (x) positions and for different spanwise positions along the y and z axis. The axis are defined figure 6; x = 0 corresponded to the outlet section of the multi-channel; y = 0 corresponded to the wake line located in the middle of the test section (75 mm from the floor wall) and z = 0 corresponded to the middle of the channels located in the center of the test section.

Figure 7 presents the evolution of CTA voltage fluctuations along particular lines of the test section. The differences in CTA fluctuations for same x position and different y and z positions were large for x/m < 20. In this region, highest CTA fluctuations were measured for y = 2 mm. From the streamwise position x/m of about 30, the difference in CTA fluctuations for different y and z position was very weak. It was then assumed that homogeneity of the turbulent filed was reached for this position.

An interesting feature of the turbulent field can be observed for the streamwise positions around x/m = 20 where a local increase in the fluctuations was measured. It could also be noted that the streamwise fluctuations decay was stronger downstream of this point. This point corresponded to the end of cone 1, see figure 4(a). It could be argued that the two Mach waves marked figure 4(a) were sufficiently strong to perturb the turbulent field. At this position, turbulent field behaved as if it was in presence of an interaction with a weak shock wave, see Jacquin et al. (1991).

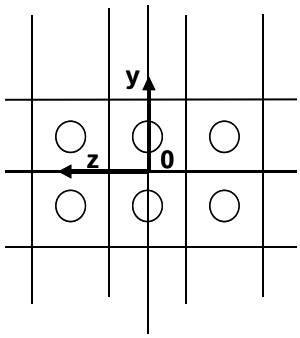

Figure 6: Definition of the y and z axis.

Using simplified CTA data reduction explained section I.C., longitudinal velocity fluctuations decay could be estimated in the assumed homogeneous part of the supersonic flow, x/m > 25–30, see figure 8. Hot-wire measurements showed the longitudinal turbulent intensity decayed with downstream distance following a power law. The exponent of the decay law was –2, which was significantly higher than the one obtained with the multi-nozzle alone, i.e. –0.79, and the one reported by Blin (1993) with a grid of similar dimension in a supersonic flow. Comte-Bellot and Corssin (1966) found values around –1.2 for subsonic decaying turbulence. For comparison, the decay law with the –0.8 exponent was reported on figure 8.The high value of the exponent could be partly explained by the interaction of the turbulent field with weak shock waves. The change in turbulent fluctuations decay could be directly related to a significant increase in the dissipation rate.

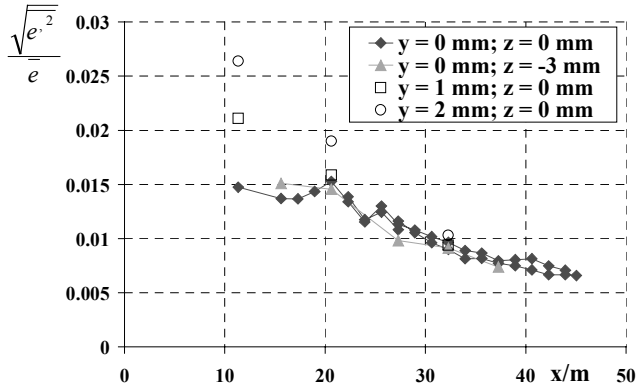

Figure 7: Repartition of CTA voltage fluctuations in the test section

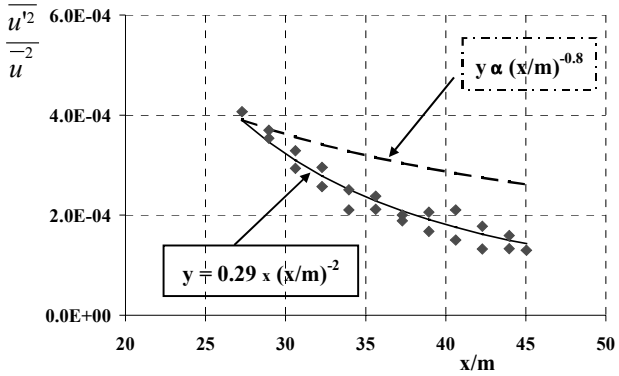

Figure 8: Velocity fluctuations decay in the assumed homogeneous part of the turbulent flow.

The isotropy of the turbulent field remained an important feature of the flow to be qualified. This is a very delicate task to undertake in that kind of flow. With the multi-nozzle alone, LDV measurements were performed to estimate the anisotropy ratio, $\frac{\overline{u'^2}}{\overline{v'^2}}$, Barre et al. (1996). This ratio was found to be close to unity for x/m > 20. Those LDV measurements also permitted to give an estimate to the correlation coefficient between longitudinal to lateral velocity fluctuations, $\overline{u'\cdot v'} \approx 0$. Similar results were found by Blin (1993) in similar flow conditions. Such measurements were not performed in this study. However, inclined hot-wire measurements were performed at the position x/m = 31 that proved that the term $\frac{\overline{(\rho\cdot u)'\cdot v'}}{\overline{\rho}\cdot\overline{u}^2}$ was zero in the limit of measurements precision and that $\overline{v'^2}=\overline{w'^2}$. Measurements with inclined hot-wire could allow the determination of $\frac{\overline{v'^2}}{\overline{u'^2}}$. These are delicate and result in important uncertainty. They were then not performed in the present study.

Therefore, on the basis of these results, we assumed that, from x/m = 30, a homogeneous mean flow was obtained that convects decaying homogeneous and isotropic turbulence.

Assuming isotropy, from the longitudinal variation of $\frac{\overline{u'^2}}{\overline{u}^2}$, dissipation rate could be estimated. The differential equation for energy decay rate in isotropic turbulence is:

$$\frac{1}{2}\cdot\frac{dq^2}{dt}=-\varepsilon \qquad \text{(Eq.1)}$$

with $q^2=3\cdot\overline{u'^2}$. Using Taylor hypothesis, Equation 1 reads:

$$\varepsilon=-\frac{3}{2}\cdot\overline{u}^3\cdot\frac{d}{dx}\left(\frac{\overline{u'^2}}{\overline{u}^2}\right) \qquad \text{(Eq. 2)}$$

With Equation 2 and the power law deduced from data figure 8, important turbulent quantities could be estimated. In order to know the inflow conditions for the shock/turbulence interaction problem, these quantities had to be computed just upstream of the position of the normal shock (values are given in table 1). The next step of this study was then to define a new shock generator geometry.

IV. DETERMINATION OF AN OPTIMUM SHOCK GENERATOR SYSTEM

Normal shock was created at the center of the test section using a Mach effect (shock intersection system), see figure 2. It is important to note that the two wedges forming the shock generator had to be located outside of the boundary layers that develop on the tunnel wall to prevent unsteadiness of the shock intersection system.

In the design of the shock generators, two parameters are relevant: the angle between inclined walls that create inclined shocks and the flow direction and the length of the inclined walls. Computations assuming inviscid flow were undertaken to evaluate the influence of these two parameters on the height (length in y direction) of the normal shock and on the longitudinal velocity gradient downstream of the normal shock. They showed that the angle and the length of the inclined walls had to be as long as possible to generate a high normal shock and a weak acceleration region downstream. However, high inclination would create strong inclined shock that would be highly unstable due to unsteady separation problem. On the other hand, long inclined wall would create an important section blockage in the test section and could make the wind tunnel impossible to start. Computations showed a satisfactory normal shock could be obtained with an inclination of 20° and an inclined wall length of 33 mm. This geometrical configuration was possible to reproduce in the wind tunnel in increasing the inclination of the shock generator after the starting of a run. Actually, due to hysteretic effect, the wind tunnel could accept blockage during a run that otherwise would have made it impossible to start if imposed before the run. Then a device was built that allowed the starting of a run with a reduced inclination of 15° and afterwards, the angle was increased up to 20 °. Figure 9 presents a Schlieren picture of the flow with a Mach effect. The shock generator was located in the test section so that the entire normal shock was in cone 2.

Mach waves could still be seen on figure 9 and the white arrow shows the end of cone 1, cf. figure 4(a). Mach waves were considerably damped in the region just upstream of the normal shock and were hardly noticeable. Two vertical segments could actually be seen in the region of the normal shock figure 9. The right segment corresponded to the normal shock. It clearly originated from the two triple intersection

points from which extended faint horizontal slipstreams. The left segment that was slightly bent corresponded to the impact of the normal shock on the glass wall and its interaction with the boundary layer. Inclination higher than 20° leaded to bent and unstable normal shock observable with spark-Schlieren pictures. With an angle of 20°, the transverse length of the normal shock was about 22 mm (to be compared with the 15 mm in the previous configuration, Barre et al. (1996)). The normal shock position was fixed at x/m = 32. Measurements in the downstream subsonic region showed the longitudinal velocity gradient was still significant, about 5500 s^{-1}.

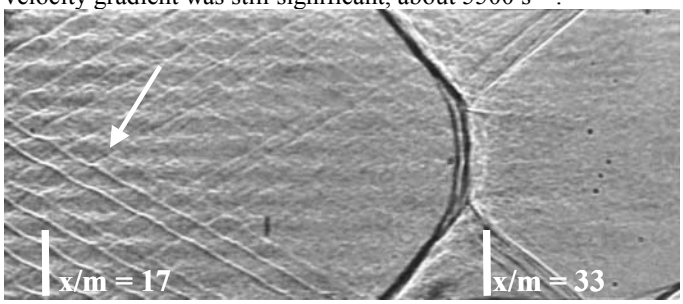

Figure 9: Spark-Schlieren picture (10 μs exposure time) of the Mach effect at Mach 2.05 (the flow is from left to right)

V. CONCLUSIONS AND FUTURE WORK

Once the position of the normal shock was fixed with the new shock generator system, detailed qualification of the turbulent supersonic field downstream of the ensemble "multi-nozzle+multi-channel" reported in section III permitted to compute important turbulent quantities before the interaction with the shock. These quantities were computed for x/m = 32, see table 1. They were compared to those obtained in the previous configuration with the multi-nozzle alone and reported in AGARDograph–AR-345. The relative turbulence intensity was defined as $\frac{\sqrt{q^2}}{\bar{u}}$, the Taylor micro-scale λ as: $\lambda=\sqrt{\frac{15\cdot\nu\cdot\overline{u'^2}}{\varepsilon}}$ and the Kolmogorov length-scale as: $\eta=(\frac{\nu^3}{\varepsilon})^{1/4}$.

With the introduction of the multi-channel, the level of longitudinal velocity fluctuations was highly increased in the downstream supersonic flow. At x/m = 32, $\frac{\sqrt{\overline{u'^2}}}{\bar{u}}$ ≈ 0.3% with the multi-nozzle and $\frac{\sqrt{\overline{u'^2}}}{\bar{u}}$ = 1.7% with the new ensemble "multi-nozzle+multi-channel". The only change in the mean flow velocity (from $\bar{u}$ = 550 m/s with the multi-nozzle to $\bar{u}$ = 505 m/s with the introduction of the multi-channel) cannot account for the observed difference. The wakes downstream of the multi-channel were more pronounced and the flow became homogeneous as far as turbulent and mean quantities were concerned, on a distance comparable to these obtained with the multi-nozzle and in subsonic grid flow.

	Multi-nozzle	Multi-nozzle + Multi-channel
Turbulent kinetic energy (m^2/s^2)	2.02	101.9
Relative turbulence intensity	0.004	0.028
Dissipation rate (m^2/s^3)	1.91×10^{3}	5.20×10^{5}
Taylor micro-scale (m)	0.79×10^{-3}	0.44×10^{-3}
Kolmogorov length-scale (m)	1.0×10^{-4}	0.37×10^{-4}
Micro-scale Reynolds number	15.5	36.6
Turbulent Mach number	0.006	0.033
Longitudinal integral scale (m)	3.4×10^{-3}	3.7×10^{-3}

Table 1: Initial conditions at the shock position.

The aim of the study was then fulfilled. On the basis of the previous experimental set-up, a new turbulence generator in supersonic flow was developed that create a stronger homogeneous (assumed isotropic) turbulent field. It was possible to fix a large normal shock in the center of the test section where Mach waves were significantly reduced. Important turbulent quantities were determined just upstream of the shock. The inflow conditions for the shock/turbulence interaction problem were therefore well defined. However, as far as turbulence modes were concerned, there is still some work to be done.

The next step in this research program is to undertake hot-wire measurements using fluctuations diagram techniques, see Kovasnay (1953). Such measurements will be performed upstream and downstream of the shock to gain further insights into the behavior of the turbulence modes through a shock. Currently, Constant Current Anemometer is being used in the laboratory with an original procedure to measure turbulent fluctuations: the raw non-compensated CCA signal is directly acquired and the signal compensation is made numerically after acquisition. Preliminary tests have shown a frequency bandwidth of the order of 150 – 200 kHz in the supersonic and transonic regime can be reached for all overheats ratio.

ACKNOWLEDGMENTS

The research on the shock/turbulence interaction problem has been supported by the Commissariat à l'Energie Atomique (CEA) through grant CEA/DAM 8M3371/PB-82 and 9M5890/AB-H2. The authors would like to acknowledge Dr. Gérard DURY who was involved in the first part of this project and Dr. Dominique AYMER DE LA CHEVALERIE in the computational help for the shock generator design.

REFERENCES

AGARDograph-AR-345, "A selection of test cases for the validation of Large-Eddy Simulations of turbulent flows", 1998.

Andreopoulos Y., Agui J.H., Briassulis G., "Shock-wave-turbulence interactions", Annu. Rev. Fluid Mech., 32, 309-345, 2000.

Barre S., Alem D. and Bonnet J-P, "Experimental study of a normal shock/homogeneous turbulence interaction", AIAA Journal, vol.34(5), 968-974, 1996.

Blin E. "Etude expérimentale de l'interaction entre une turbulence libre et une onde de choc", PhD dissertation, Université Paris VI, Paris, France, 1993.

Comte-Bellot G. and Corssin S., "The use of contraction to improve the isotropy of grid-generated turbulence", J. Fluid Mech., vol. 25, 657-682, 1966.

Debiève J-F and Lacharme J-P., "A shock wave/free turbulence interaction", Turbulent Shear Layer/shock wave interaction", edited by J. Délery, Springer-Verlag, Berlin, 1986.

Jacquin L., Blin E. and Geffroy P., "Experiments on free turbulence/shock wave interaction", 8th Symposium on Turbulent Shear Flows, TU Munich, Germany, 1991.

Kovasnay L.S.G., "Turbulence in supersonic flow", Journal of the Aeronautical Sciences, vol. 20(10), 657-674, 1953.

Ribner H.S. "Shock-turbulence interaction and the generation of noise", NACA TN-3255, 1954.

Smits A.J. and Dussauge J-P, "Hot-wire anemometry in supersonic flow", AGARDograph 24, 1989.